DOI: 10.1002/ejic.201100125

Zn^{II}–2,2′:6′,2′′-Terpyridine-Based Complex as Fluorescent Chemosensor for PPi, AMP and ADP

Priyadip Das,[a] Amrita Ghosh,[a] Manoj K. Kesharwani,[a] Vadde Ramu,[a] Bishwajit Ganguly,*[a] and Amitava Das*[a]

Keywords: Chemosensors / Zinc / Density functional calculations / Fluorescent probes / Bioinorganic chemistry

A new Zn^{II}–2,2′:6′,2′′-terpyridine complex, derivatized with a coumarin moiety (**L_1Zn**), acts as a fluorescent chemosensor for different biologically important phosphates like PPi, AMP and ADP in mixed aqueous media. Depending on the proportion of the aqueous fraction present in the solvent mixture, **L_1Zn** shows a preference for different phosphate moieties at physiological pH. In an aqueous acetonitrile (2:3, v/v) medium this reagent shows a preference for AMP as compared to ADP, ATP and PPi. The binding affinities of **L_1Zn** with different phosphate ions and associated shifts in the electronic spectra were rationalized by DFT calculations. Such an example of a receptor that is selective for AMP under physiological conditions is rare in the literature.

Introduction

The selective recognition and sensing of biologically important phosphate ions have been the focal point of current research because these ions play crucial role(s) in various metabolic processes.[1–4] More importantly adenosine triphosphate (ATP) and pyrophosphate (PPi) are involved in energy transduction in organism-controlling metabolic processes by participation in enzymatic reactions, e.g. DNA replication, etc.[5–7] Furthermore, the detection of PPi is important in real-time DNA sequencing methods,[8] as well as in cancer research and is formed by the hydrolysis of ATP into adenosine monophosphate (AMP) in cells. AMP and adenosine diphosphate (ADP) are well known to play a crucial role in the energy cycle, as well as in various other biological processes.[9] Accordingly, detection and discrimination of these phosphates are important for evaluating the generation of each of these ions during various biological processes and clarifying their roles in these processes. Among various methodologies adopted for developing sensor molecules for anionic analytes in aqueous environments, metal ion–anion coordination is recognized as one of the most popular for ions with a high hydration energy, e.g. fluoride, various phosphates, acetate ions. In this regard, the Zn^{2+} complex with vacant coordination sites is significant as the Zn^{2+} ion generally has higher affinity towards phosphate functionality. Higher affinity and stronger Zn^{II}–phosphate binding is expected to be reflected in the more pronounced influence on the molecular orbital energy levels and thereby on the output spectral response. Besides this, Zn^{2+} does not exhibit any emission quenching effects to fluorophore because of its electronic ($3d^{10}4s^0$) configuration. Thus, examples of the Zn^{2+}-based chemosensors for recognition of biological phosphates, which work either in aqueous environments or under physiological conditions, are relatively more common in the literature than those that work on the hydrogen-bonded adduct formation procedure.[10,11] However, examples of an appropriate receptor that shows preferential binding affinity towards AMP or PPi, compared to other common anions like F^-, Cl^-, Br^-, I^-, NO_3^-, CH_3COO^-, $C_6H_5COO^-$, SO_4^{2-}, HSO_4^-, $H_2PO_4^-$ and other biologically important phosphate ions like ATP, CTP, ADP under different mixed aqueous buffer-solvent environments, are scarce in the literature. This promoted us to design and synthesize Zn^{II} complexes as a fluorescent probe for different phosphates like AMP and PPi. Most of the Zn^{II} complexes, which are used as the receptor for phosphate ions, are generally either various derivatives of Zn^{II}–dipicolylamine[10,11a–11h] or Cu^{II}–dipicolylamine,[11i,11j] barring one recent reference where Zn^{II}–cyclen (1,4,7,10-tetraazacyclododecane) is reported to show comparable affinity towards ATP and PPi.[12a] There are only few examples available in the literature where Cu^{II}/Cd^{II}–cyclen derivatives are used as receptors for AMP/PPi.[12,13a] Though the Cu^{II} complex shows specificity toward PPi, observed binding affinity was not appreciable; while the anion binding response for the Cd^{II}–cyclen derivative works on displacement phenomena and lacks any specificity towards PPi. In a recent report, Gao et al. have shown that a dizinc(II)–cyclen derivative could also be used for specific binding to deoxythymidine and thymidylylthymidine.[13b] In this article we report synthetic methodology, characterization and binding stud-

[a] Central Salt & Marine Chemicals Research Institute (CSIR), Bhavnagar, 364002 Gujarat, India
Fax: +91-278-2567562
E-mail: amitava@csmcri.org
ganguly@csmcri.org

Supporting information for this article is available on the WWW under http://dx.doi.org/10.1002/ejic.201100125.

ies of a newly synthesized Zn^{II}–tpy derivative (tpy is 2,2′:6′,2′′-terpyridine) (**L_1Zn**) as an anion receptor (Scheme 1). This shows an appreciable preference towards PPi, compared to other anions like F^-, Cl^-, Br^-, I^-, NO_3^-, CH_3COO^-, $C_6H_5COO^-$, SO_4^{2-}, HSO_4^-, $HP_2O_7^{3-}$, $H_2PO_4^-$ in an aq.·HEPES buffer/CH_3CN (1:4, v/v) medium; while in solvent media with a higher proportion of protic solvent [aq. HEPES/CH_3CN buffer, 2:3 (v/v)] **L_1Zn** was found to bind specifically to AMP and ADP compared with ATP, CTP, PPi and all the above mentioned ions. The experimental observations have been corroborated by density functional theory (DFT) calculations.

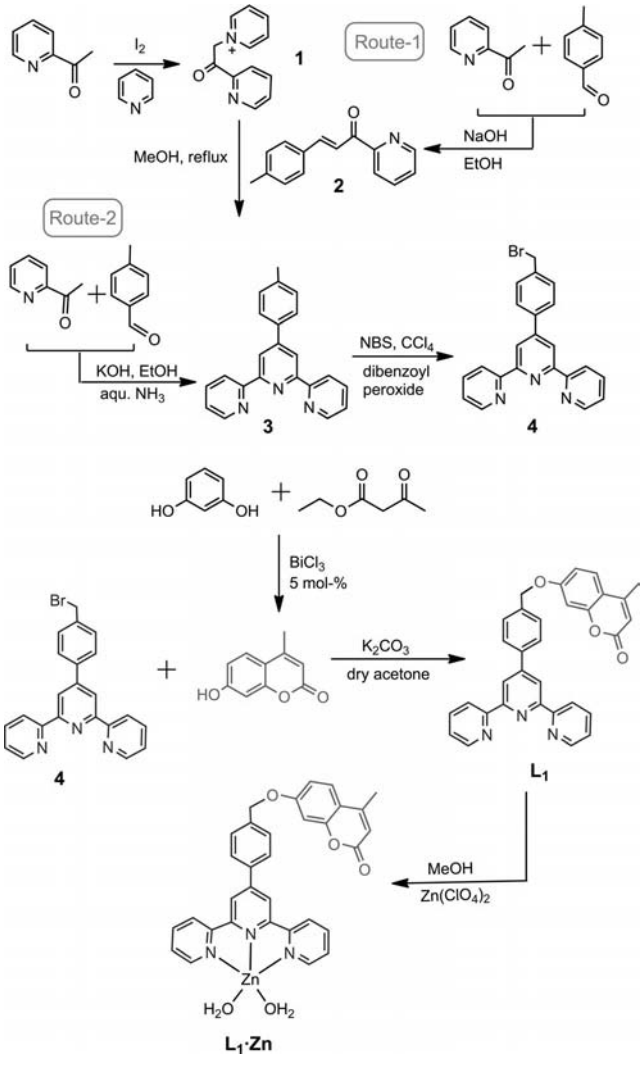

Scheme 1.

Results and Discussion

Pyridasyl pyridinium iodide salt and (*E*)-3-(4-methylphenyl)-1-(pyrid-2-yl)prop-2-enone were synthesized and these two reagents were eventually allowed to react for the synthesis of 4′-(*p*-methylphenyl)-2,2′:6′,6′′-terpyridine following previously reported methodology.[14] This terpyridyl derivative was also synthesized from an alternate methodology (Scheme 1) following a one-step procedure by reacting 2 mol-equiv. of 2-acetylpyridine and 1 mol-equiv. of 4-methylbenzaldehyde.[15] This was subjected to the free radical bromination reaction using NBS as the brominating agent.[16] 4′-[*p*-(Bromomethyl)phenyl]-2,2′:6′,6′′-terpyridine was isolated in reasonably good yield and was allowed to react with presynthesized 7-hydroxy-4-methylcoumarin in the presence of K_2CO_3 and a catalytic amount of 18-crown-6 in dry acetone to yield **L_1** in reasonable yield (Scheme 1).[17] This was allowed to react with $Zn(ClO_4)_2$ at room temperature to yield the desired compound. For simplicity **$L_1Zn(H_2O)_2$** is represented as **L_1Zn**.

Spectral Behaviour of L_1 and L_1Zn

The electronic spectrum recorded for **L_1** in H_2O/CH_3CN (1:4, v/v) (Figure S1) shows three absorption maxima at 251 ($\varepsilon = 2.3 \times 10^4$ M^{-1} cm^{-1}), 278 ($\varepsilon = 2.92 \times 10^4$ M^{-1} cm^{-1}) and 313 nm (broad absorption band, $\varepsilon = 1.7 \times 10^4$ M^{-1} cm^{-1}). These absorption bands could be assigned to various $\pi \rightarrow \pi^*$ transitions, while a weaker $n \rightarrow \pi^*$ transition was submerged under a stronger $\pi \rightarrow \pi^*$ transition. Among these, the band at 251 nm could be assigned to the tpy-based $n \rightarrow \pi^*$ transition; while bands at longer wavelengths are presumably from the tpy or coumarin-based $\pi \rightarrow \pi^*$ transition (for 278 nm transition) or inter-component $\pi_{coumarin/tpy} \rightarrow \pi_{tpy/coumarin}^*$-based transitions (for 313 nm transition). Luminescence spectra recorded for L_1 on excitation at either 278 or 313 nm show similar spectral patterns with an emission maximum at 380 nm (Figure 1). Two analogous individual chromophores, 4′-(*p*-methoxyphenyl)-2,2′:6′,6′′-terpyridine (L) (Figure S4) and 7-ethoxy-4-methylcoumarin (Figure S14), show strong and small broad emission bands at ca. 390 (λ_{abs}^{max} = 284 nm) and 360 nm (λ_{abs}^{max} = 315 nm), respectively. Data reported earlier for 7-methoxy-4-methylcoumarin is similar to that evaluated for the ethoxy derivative.[18] Thus, for L_1, the emission band around 380 nm (with λ_{ext} = 278 or 313 nm) primarily could be the combination of 2,2′:6′,6′′-terpyridine and coumarin-centre based emission. On binding to the Zn^{2+} ion through the coordinating terpyridine unit in **L_1Zn**, two absorption bands appeared at 286 and 325 nm, along with a distinct hump at around 347 nm in the H_2O/CH_3CN (1:4, v/v) solvent medium (Figure 1). The small red shift of the absorption bands could be explained based on the decrease in the LUMO energy on binding to the cationic Zn^{II} centre and presumably this could be attributed to a charge transfer (CT) spectrum with coumarin as the donor and the Zn^{II}-bound terpyridyl unit as the acceptor fragment. This presumption was further supported by the results of the density functional studies (vide infra). Fluorescence spectra for **L_1Zn** show two emission bands at 370 and 456 nm in CH_3CN (Figure 1) on excitation at λ_{ext} = 315 nm, while red-shifted emission bands appear at 381 and 467 (broad) in the more polar H_2O/CH_3CN (1:4, v/v) medium (Figure 1). A further red shift for each of these bands (386 nm and 480 nm) was observed on increasing the medium polarity

with an increase in the proportion of water [H_2O/CH_3CN (2:3, v/v)] in the mixed solvent medium (Figure 1). The red-shift of the emission bands on increasing solvent polarity suggests that the excited state for **L_1Zn** is more polar as compared to the ground state. Further, excitation spectra recorded for **L_1Zn** using λ_{ems} of 379 and 460 nm revealed that the excitation spectral patterns are different (Figure S5). These indicate that excited states, which are responsible for the emission bands with maxima at 379 and 460 nm, are different. New emission maxima at ca. 460 nm could be assigned to the CT process involving the donor coumarin fragment and acceptor terpyridine moiety bound to the Zn^{II} centre.

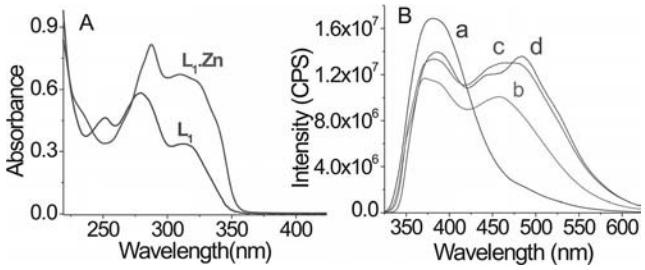

Figure 1. (A) Absorption spectra of **L_1** and **L_1Zn** (2.15×10^{-5} M) in an aq. HEPES buffer/CH_3CN (1:4, v/v) medium. (B) (a) Fluorescence spectra of **L_1** (2.15×10^{-5} M) in an aq. HEPES buffer/CH_3CN (1:4, v/v) medium, (b) **L_1Zn** (2.15×10^{-5} M) in a CH_3CN (c) in an aq. HEPES buffer/CH_3CN (pH = 7.4) (1:4, v/v) (d) in an aq. HEPES buffer/CH_3CN (pH = 7.4) (2:3, v/v) medium using λ_{ext} = 315 nm.

Fluorescence decay traces recorded for **LZn**, 7-ethoxy-4-methylcoumarin and **L_1Zn** in an air-equilibrated acetonitrile solution, following excitation with either a 340 nm or 280 nm LED source and the respective decay constants are provided in Table 1. It is evident from Table 1 that on excitation of **L_1Zn** with the 280-nm LED (for λ_{mon} = 465 nm), the decay component for the coumarin fragment is higher compared to the situation where the 340 nm LED is used. The longer and larger component of 2.002 ns (for λ_{ext} = 280 nm) or 1.74 ns (for λ_{ext} = 340 nm) could be attributed to the emission decay of the CT state. This is in agreement with the coumarin fragment showing less excitation at 340 than at 280 nm.

The emission decay constant for the analogous coumarin component (4-hydroxy-7-methoxycoumarin) is reported as τ = 0.13 ns (λ_{ext} = 310 nm and λ_{mon} = 370 nm) in dioxone for the $^1(\pi–\pi)^*$-based emission.[18] For **LZn** a single time constant of about 4.465 ns was obtained experimentally. These values clearly indicate that for **L_1Zn** the emissive state associated with the emission band maxima at 460 nm is different from the one that is associated with the emission band maxima at 379 nm. The CT nature of the emission band at 460 nm is well supported by the results of the density functional calculations and is discussed later.

Optical absorption spectra for **L_1Zn** were recorded in the absence and presence of various anionic analytes such as $F^–$, $Cl^–$, $Br^–$, $I^–$, $NO_3^–$, $CH_3COO^–$, $C_6H_5COO^–$, $SO_4^{2–}$, $HSO_4^–$, $H_2PO_4^–$ and $HP_2O_7^{3–}$ (PPi) in an acetonitrile solution. Apart from $I^–$, $NO_3^–$, $HSO_4^–$ a detectable change in electronic spectral patterns (Figure S6) could be observed for all the other anions mentioned. For most of the anions used, including PPi, a small blue shift in the absorption band was observed. However, for emission spectra recorded in an acetonitrile medium, a significant change (λ_{ext} = 314 nm) was observed when PPi, $H_2PO_4^–$, $CH_3COO^–$, $F^–$ and $Cl^–$ ion was added; while no such change was observed for all the other anions studied. The emission band at ca. 460 nm tends to disappear, and enhancements in emission bands at around 379 nm were observed (Figure S7). This indicates that binding of these anions to the Zn^{II} centre is responsible for the complete quenching of the particular excited state that is related to the 460 nm emission band and is not in equilibrium with the other excited state that accounts for the emission maximum at 379 nm. This emission band is believed to be an intra-ligand (tpy/coumarin)-based charge transfer transition in nature. For spectral studies in an aq. HEPES buffer/CH_3CN (pH = 7.4) (1:4, v/v) medium, appreciable changes were observed only for $HP_2O_7^{3–}$ (Figure 2). In the electronic spectra a small blue shift was observed (Figure 2, A); while significant changes were observed in the emission spectra (Figure 2, B) in presence of $HP_2O_7^{3–}$. Presumably, the higher energy of hydration for $F^–$ and $RCOO^–$ does not allow these anions to coordinate to the Zn^{II} centre; while lower charge density of the respective anion like $Cl^–$, $Br^–$, $I^–$, $NO_3^–$, $SO_4^{2–}$ and $HSO_4^–$ presumably accounts for the weaker or negligible binding to the Zn^{II}-based receptor.[19] Insignificant change in the emission spectra was also observed in the presence of excess $H_2PO_4^–$. Attempts to monitor the emission spectral response in presence of added AMP, ADP, CTP, and ATP was also not successful as these phosphates were found to be sparingly soluble in this solvent composition [aq. HEPES buffer/CH_3CN, 1:4 (v/v)].

An associated binding constant for the formation of **L_1Zn**–PPi was evalulated using emission intensity data (at

Table 1. Time resolved emission decay constants for **L_1Zn** and analogous components in an air-equilibrated acetonitrile solution at 295 K.

	λ_{ext} (nm)	λ_{379}^{Mon} (nm)	λ_{460}^{Mon} (nm)
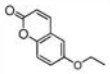	280[a]	$\tau_1 \leq 0.127$ ns (96.8 %); τ_2 = 1.27 (3.2 %); χ^2 = 1.23	$\tau_1 \leq 0.12$ ns (94.8); τ_2 = 2.19 ns (5.2 %); χ^2 = 1.05
LZn	280	τ_1 = 4.42 ns; χ^2 = 0.94	τ_1 = 4.464 ns; χ^2 = 1.125
L_1Zn	280	$\tau_1 \leq 0.162$ ns (36.8 %); τ_2 = 2.35 ns (63.1 %); χ^2 = 1.280	$\tau_1 \leq 0.112$ ns (20%); τ_2 = 2.002 ns (80%); χ^2 = 1.031
	340	$\tau_1 \leq 0.143$ ns; χ^2 = 0.9	$\tau_1 \leq 0.111$ ns (7.5%); τ_2 = 1.745 ns (92.5%); χ^2 = 0.93

[a] The emission decay constant reported for the analogous compound 4-methyl-7-methoxycoumarin in dioxane is 0.13 ns.[18]

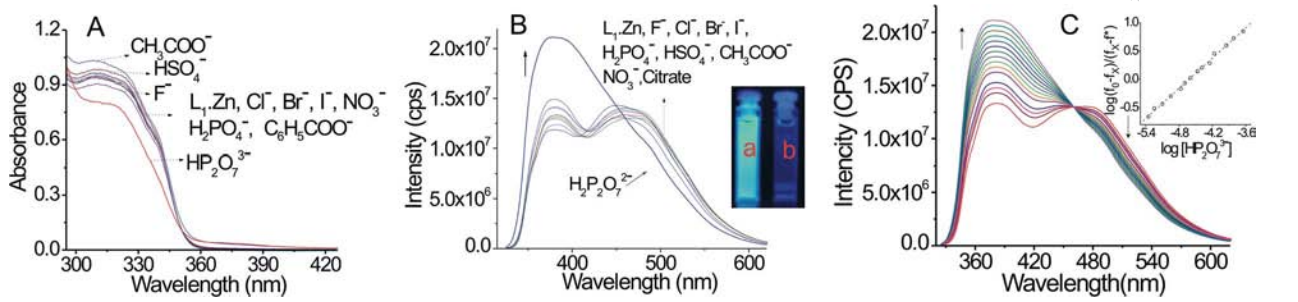

Figure 2. (A) Absorption and (B) emission spectra of the chemosensor (**L_1Zn**) at 2.15×10^{-5} M in the presence of different anions at 8×10^{-4} M in an aq. HEPES buffer/CH_3CN (pH = 7.4) (1:4, v/v) medium; (C) fluorescence spectra of **L_1Zn** (2.15×10^{-5} M) in an aq. HEPES buffer/CH_3CN (pH = 7.4) (1:4, v/v) medium in the presence of an increasing concentration of PPi (0–8×10^{-4} M), λ_{ext} = 315 nm; inset: double-logarithmic plot for the above spectral change at 379 nm for λ_{ext} = 315 nm. Inset: photographs of the quartz cuvette showing fluorescence of (A) **L_1Zn** and (B) **L_1Zn**–PPi in an aq. HEPES buffer/CH_3CN (1:4, v/v) medium after exposing solutions to UV radiation.

λ_{ems} = 379 nm) obtained from the systematic fluorescence titration profile (Figure 2, C). The slope of the double-logarithmic plot [see Equation (2) in the Exp. Section] obtained from the experimental data, represents the number of binding sites or stoichiometry (n) and this was found to be one. The value for log K_d was obtained from log([A^-]) at log[$(F_0 - F_x)/(F_x - F_\alpha)$] = 0. The solid line in the inset of Figure 2, C represents the best fit of the plot with a regression coefficient value of 0.998. The reciprocal of K_d is the binding constant (K_b) and was evaluated from this plot as $(2.2 \pm 0.18) \times 10^5$ M^{-1}. A similar 1:1 binding stoichiometry for PPi was also evaluated from the titration profile (Figure S8). The binding constant was also determined for $H_2PO_4^-$ in an aq. HEPES buffer/CH_3CN (1:4, v/v) medium and was found to be 98 ± 0.8 M^{-1} under identical conditions. Stronger electrostatic interactions between the cationic Zn^{2+} centre and $HP_2O_7^{3-}$, compared with $H_2PO_4^-$, could be attributed to the higher affinity of PPi towards the receptor **L_1Zn**. Independent interference studies revealed that changes in fluorescence due to the addition of 5.0×10^{-4} M of PPi remained unaffected even in the presence of 10 mol-equiv. of $H_2PO_4^-$ and other common anions mentioned above. Thus, by probing the fluorescence output as the response signal, **L_1Zn** could be used as a fluorogenic sensor molecule for biologically important pyrophosphate ions in aq. HEPES buffer/CH_3CN (1:4, v/v) medium. The small blue shift in the absorption spectra for **L_1Zn** on binding to PPi can be explained by DFT calculations and is discussed later.

In order to understand the nature of binding of the PPi ion to the Zn^{II} centre of **L_1Zn**, we recorded the ^{31}P NMR spectrum (Figure 3) of the tetrabutylammonioum salt of pyrophosphate in the absence and presence of 1.5 mol-equiv. of **L_1Zn** in CD_3CN. ^{31}P NMR spectra recorded for PPi suggest that both P atoms present in the PPi moiety are equivalent, however, on binding to the Zn^{II} centre a pronounced upfield shift was observed for the P_α atom as compared to that for the P_β atom.[11c,11e] This observation may be explained using two different models. According to the first model, a strong Zn^{II}–OP_α and a much weaker Zn^{II}–OP_β binding accounts for the less appreciable upfield shift for P_β in the ^{31}P NMR spectra; while for the second model, PPi is proposed to bind to the Zn^{II} centre only through $P_\alpha O$ and this strong binding induces an upfield shift for the P_β atom in bound PPi. However, strong binding of PPi to the Zn^{II} centre of **L_1Zn** as compared to $H_2PO_4^-$ could be better explained by the proposed first model, i.e., binding of PPi to the Zn^{II} centre of **L_1Zn** through a stable six-membered chelate. Further experiments revealed that spectral patterns for **L_1Zn** in the presence of 2 mol-equiv. of PPi remained unchanged even in the presence of 10 mol-equiv. of other anions (F^-, Cl^-, Br^-, I^-, NO_3^-, CH_3COO^-, $C_6H_5COO^-$, SO_4^{2-}, HSO_4^- and $H_2PO_4^-$). This confirmed the specificity of **L_1Zn** towards PPi in presence of these anions in an aq. HEPES buffer/CH_3CN (1:4, v/v) medium.

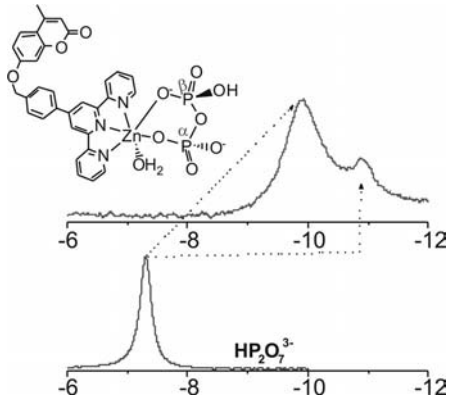

Figure 3. Partial ^{31}P NMR (CD_3CN) spectra for PPi in the absence and presence of 1.5 equiv. of **L_1Zn**.

In order to check the binding affinity of this Zn^{II}-based receptor unit towards other biologically important phosphates (e.g. ATP, CTP, ADP and AMP) we needed to increase the proportion of the water or HEPES buffer in the composition of the mixed solvent. Optical (Figure 4, A) and fluorescence (Figure 4, B) spectral responses of **L_1Zn** towards these anions, along with all other anions (F^-, Cl^-, Br^-, I^-, NO_3^-, CH_3COO^-, $C_6H_5COO^-$, SO_4^{2-}, HSO_4^- and $H_2PO_4^-$) mentioned earlier, were checked in an aq. HEPES buffer/CH_3CN (2:3, v/v) medium (pH = 7.4) (Figure 4).

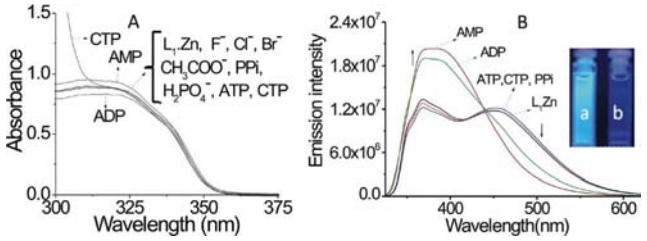

Figure 4. (A) Absorption and (B) emission spectra of $\mathbf{L_1Zn}$ (2.15×10^{-5} M) in the absence and presence of different anions (8.0×10^{-4} M) in an aq. HEPES buffer/CH_3CN (2:3, v/v) medium (pH = 7.4); inset: photographs of the quartz cuvette showing fluorescence of (a) $\mathbf{L_1Zn}$ and (b) $\mathbf{L_1Zn}$–AMP in an aq. HEPES buffer/CH_3CN (2:3, v/v) medium after exposing solutions to UV radiation.

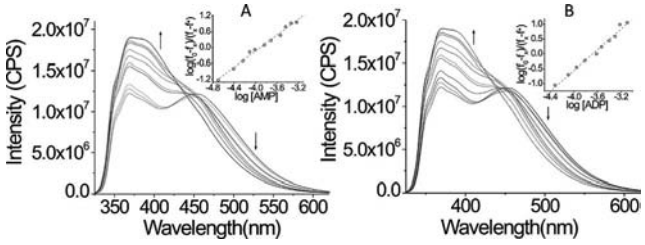

Figure 5. Fluorescence spectra of $\mathbf{L_1Zn}$ (2.15×10^{-5} M) in an aq. HEPES buffer/CH_3CN (2:3, v/v) (pH = 7.4) medium in the presence of varying (A) [AMP] = ($0–1 \times 10^{-3}$ M) and (B) [ADP] = ($0–1 \times 10^{-3}$ M). Respective inset figures reveal the double-logarithmic plot for the spectral changes at 379 nm.

No detectable change in the absorbance spectra of $\mathbf{L_1Zn}$ was evident on addition of these anionic analytes (Figure 4, A); however, emission spectral studies revealed detectable changes only for AMP and ADP (Figure 4, B). No other anions including ATP, CTP and PPi could induce either a negligible or very weak spectral change. Between AMP and ADP, emission spectral changes were more prominent for AMP. This signifies that either very weak or negligible binding of other anions, except AMP and ADP, occurs at the Zn^{II} centre of $\mathbf{L_1Zn}$. The observed preference for AMP/ADP, compared to PPi in more polar aqueous/CH_3CN (2:3, v/v) media could be explained if one considers the difference in solvation energy of various phosphates in water media. Enthalpy of solvation for $HP_2O_7^{3-}$ in water is reported to be much higher than the related monophosphate (for $H_2PO_4^-$, ΔH = 76 kcal/mol) or diphosphate ($H_3P_2O_7^-$, ΔH = 87 kcal/mol) and thus $HP_2O_7^{3-}$ prefers to remain in the solvated form rather than being coordinated to the Zn^{II} centre in $\mathbf{L_1Zn}$.[19a,20] Thus, the increase in polarity of the solvent with an increase in the proportion of water is responsible for the more extensive hydration of PPi as compared with AMP and ADP and thus loss of coordination by PPi to the Zn^{II} centre in $\mathbf{L_1Zn}$ in an aq. HEPES buffer/CH_3CN (2:3, v/v) medium. The relative affinities of AMP and ADP towards $\mathbf{L_1Zn}$ were evaluated through systematic fluorescence titration profiles using 2.15×10^{-5} M of $\mathbf{L_1Zn}$ and varying [ADP] of $0–1.0 \times 10^{-3}$ M or [AMP] of $0–9.97 \times 10^{-4}$ M; the respective sets of emission spectra with varying [AMP] and [ADP] are shown in Figure 5.

The affinity constant was evaluated from the plot of $\log[(F_0 - F_x)/(F_x - F_\alpha)]$ vs. $\log([A])$ (inset of Figure 5) using Equation (2). Solid lines shown in the inset of Figure 5 and the regression coefficient data suggest the correctness of the plots. For both the cases, a 1:1 binding stoichiometry was evident (n = 1) and the binding constants for AMP and ADP were evaluated as $(7.2 \pm 0.2) \times 10^3$ M^{-1} and $(5.1 \pm 0.25) \times 10^3$ M^{-1}, respectively, at 25 °C in an aq. HEPES buffer/CH_3CN (2:3 (v/v), pH = 7.4) medium. Affinity constants for PPi towards $\mathbf{L_1Zn}$ were also evaluated and were found to be 121 ± 7 M^{-1}. No detectable change in the fluorescence spectral pattern for ATP/CTP prevented the evaluation of the respective binding affinities. Thus, the observed relative binding affinity of $\mathbf{L_1Zn}$ towards three different nucleotides follows the order, $K_{AMP} > K_{ADP} > K_{PPi} >> K_{ATP}$. This could be best explained if one considers a shorter chain length of AMP, which allows a more efficient π–π stacking interaction between the adenine moiety and the nearly planar terpyridine group of the receptor fragment ($\mathbf{L_1Zn}$), as compared with that in the case of ADP or ATP. Such an explanation for the Hg^{II}/Cu^{II}-based receptor for preferential binding to GMP is reported earlier.[21]

A detailed literature survey on the receptors that could preferentially bind to AMP results in only a few reports.[22] In the first report, Kimura et al. have shown that different protonated forms of azamacrocycles could bind ATP, ADP and AMP through hydrogen bond formation involving the anionic $O_{Phosphate}$ of the respective nucleotide and the $(H)N^+_{Macrocycle}$, which could be probed only by ^1H NMR spectroscopic studies.[22a] While the second one includes a Zn^{II}–dipicolylamine-based receptor that works on the displacement mechanism utilizing the weaker Zn^{II}–AMP binding as compared with Zn^{II}–catechol binding.[22b] A very recent report has described the selective binding of the other monophosphate (5′-GMP) in a mixed organic–aqueous (DMSO/H_2O, 1:4, v/v) medium,[21a] where binding of the monophosphate caused a decrease in the luminescence intensity and the binding constant was evaluated as 1.2×10^4 M^{-1}. Thus, considering available literature reports, selective binding achieved for AMP and ADP in mixed aqueous/CH_3CN (2:3, v/v) is significant.

To understand the relative binding affinity of PPi, AMP and ADP towards $\mathbf{L_1Zn}$ and the possible role of solvation in affecting the relative binding affinities/preferences, along with the nature of the observed blue shift in the absorption spectra for $\mathbf{L_1Zn}$ on coordination to PPi, DFT calculations have been performed. The molecular electrostatic potential (MESP) was calculated for $HP_2O_7^{3-}$ and the monoanionic form of AMP and ADP (salts used for studies and expected to prevail at pH = 7.4) at the BLYP/6-31G** level in both acetonitrile and aqueous phase (Figure 6). To simplify the MESP analysis, the most negative evaluated point (V_{min}) in the electron-rich regions was obtained through topography calculations. The calculated V_{min} for $HP_2O_7^{3-}$ in acetonitrile is much higher (–368.3 kcal/mol) than the monoanionic

forms of AMP (–200.8 kcal/mol) and ADP (–135.5 kcal/mol). A similar trend was also observed in the aqueous phase ($HP_2O_7^{3-}$, –369.6 kcal/mol; AMP, –200.8 kcal/mol; ADP, –136.2 kcal/mol). Thus, the MESP analysis suggests that $HP_2O_7^{3-}$ should bind strongly to **L_1Zn** compared to AMP and ADP. To compare the binding ability of $HP_2O_7^{3-}$ and AMP towards **L_1Zn**, calculations were performed using the GGA/BLYP/DNP method in both acetonitrile and water. The calculated binding energy for $HP_2O_7^{3-}$ is 13.2 kcal/mol higher than AMP in acetonitrile. However, in a solvent with high polarity (water) the difference in binding energy is only 7.2 kcal/mol, which is 6.0 kcal/mol lower than the difference in the binding energy calculated in acetonitrile.

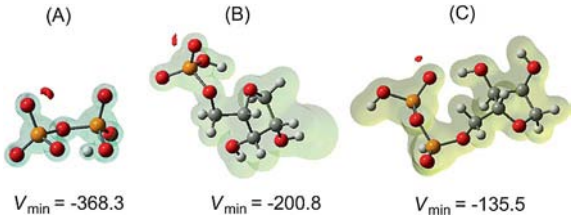

Figure 6. The MESP isosurfaces of (A) $HP_2O_7^{3-}$, (B) monoanionic AMP and (C) monoanionic ADP generated with the isosurface value of 1.25 kcal/mol in acetonitrile. The position of V_{min} is shown in red [colour code, gray: carbon, red: oxygen, yellow: phosphorus, white: hydrogen].

This reveals that the increase in polarity of solvent decreases the binding affinity of $HP_2O_7^{3-}$ towards **L_1Zn**. This coupled with higher solvation energy for PPi could actually account for either very weak or a lack of any affinity of PPi for **L_1Zn** in an aq. HEPES buffer/CH_3CN [2:3 (v/v)] medium.

Further, to understand the shift in absorption spectra of **L_1Zn** on binding with the $HP_2O_7^{3-}$ ion, calculations were performed using the GGA/BLYP/DNP method in both acetonitrile and water. The HOMO–LUMO of **L_1Zn** generated from DFT calculations in acetonitrile as the solvent are given in Figure 7 (A). The corresponding orbitals generated for the complex **L_1Zn**–$HP_2O_7^{3-}$ are given in Figure 7 (B). For **L_1Zn** the HOMO is largely located on the coumarin moiety, whereas the LUMO is largely located on the Zn^{II}-bound terpyridine group. This suggests that for the absorption spectra, intrercomponent charge transfer predominantly happens from coumarin to the Zn^{II}-bound terpyridine group. The calculated energy for this electronic transition is 2.169 eV; however, the energy for corresponding electronic transitions in **L_1Zn**–$HP_2O_7^{3-}$ is 2.541 eV. The higher transition energy in the latter case suggests the blue shift of absorption spectra after binding with $HP_2O_7^{3-}$, which is qualitatively in agreement with the experimental results. To see the effect of polarity of solvent, calculations were also performed in water at the same level of theory. The calculated results gave similar results (Figure S10) but with a slightly less difference in transition energy compared to the results obtained in acetonitrile.

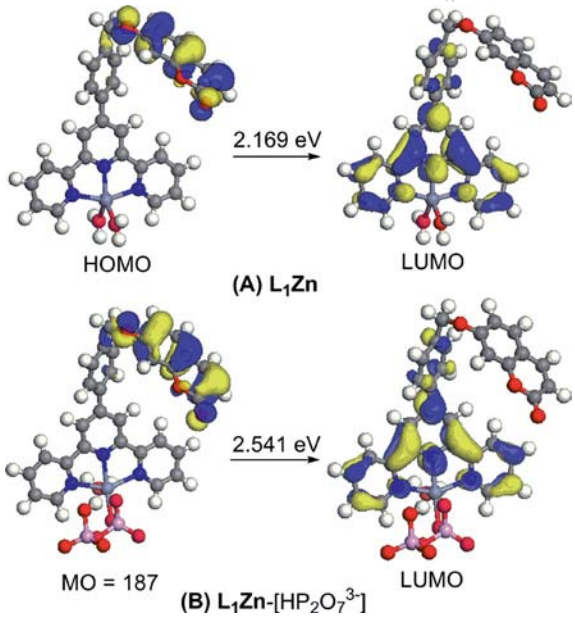

Figure 7. The frontier molecular orbitals involved in the electronic transition for (A) **L_1Zn** and (B) **L_1Zn**–[$HP_2O_7^{3-}$] calculated from the GGA/BLYP/DNP method in an acetonitrile medium [colour code, gray: carbon; red: oxygen; pink: phosphorus; blue: nitrogen; white: hydrogen].

Conclusions

In this work we have described a new Zn^{II}-based receptor molecule that could bind reversibly with various biologically important phosphate ions. In an aq. HEPES buffer/CH_3CN (1:4, v/v) medium (pH 7.4) **L_1Zn** was found to bind PPi in the presence of an excess of other common anions, like F^-, Cl^-, Br^-, I^-, NO_3^-, CH_3COO^-, $C_6H_5COO^-$, SO_4^{2-}, HSO_4^- and $H_2PO_4^-$; while in the more polar solvent environment with a higher proportion of aqueous solution, e.g. an aq. HEPES buffer/CH_3CN (2:3, v/v) medium, this receptor showed specificity towards AMP/ADP, as compared with ATP and PPi. Solvation of these anions play a crucial role and relative binding affinity changes for these anions with the increase in the proportion of the protic solvent like water in the solvent mixture. DFT calculations have been performed to rationalize the observed preferences of this Zn^{II}-based receptor towards these phosphate ions.

Experimental Section

Materials and Methods: The chemicals such as 2-acetylpyridine, 4-methylbenzaldehyde, ethyl acetoacetate, *N*-bromosuccinimide (NBS), dibenzoyl peroxide, tetrabutylammonium salts of various anions, different nucleotides (adenosine 5′-monophosphate monohydrate, adenosine 5′-diphosphate sodium salt, adenosine 5′-triphosphate disodium monohydrate and cytidine 5′-triphosphate disodium salt monohydrate) were obtained from Sigma–Aldrich and were used as received without any further purification. All the other reagents used were of reagent grade (S. D fine chemical, India) and were used as received. Pyridasyl pyridinium iodide salt, (*E*)-3-(4′′-methylphenyl)-1-(pyrid-2′-yl)prop-2-enone, 4′-(*p*-methylphenyl)-2,2′:6′,6′′-terpyridine, 4′-(*p*-methylphenyl)-2,2′:6′,6′′-ter-

pyridine, 4′-[4-(bromomethyl)phenyl]-2,2′:6′,2′′-terpyridine and **L_1**, 7-hydroxy-4-methylcoumarin were synthesized following previously reported procedures.[23] Various analytical and spectroscopic data obtained for these intermediates provided necessary supports for the proposed formulation and required purity (Supporting Information). These were used without any further purification. HPLC grade water (Fisher Scientific) was used as a solvent. Acetonitrile and acetone were used for studies and were purified through distillation following standard procedures prior to use. Elemental analysis was conducted with a 4100 elemental analyzer. FTIR spectra were recorded as KBr pellets with a Perkin–Elmer Spectra GX 2000 spectrometer. ^{1}H and ^{31}P NMR spectra were recorded with a Bruker 200 MHz (Avance-DPX 200)/500 MHz (Bruker Avance II 500) FT spectrometer. Electronic spectra were recorded with a Shimadzu UV-3101 PC spectrophotometer; while fluorescence spectra as well as time-correlated single-photon counting (TCSPC) studies were carried out using Edinburgh Instruments, Model H5773-03, fitted with a blue-sensitive photomultiplier.

Spectrophotometric Study: An aqueous HEPES buffer solution was used for maintaining a pH of 7.4. A 1.07×10^{-4} M solution of **L_1Zn** in an aq. HEPES buffer/CH3CN (pH = 7.4) and two different buffer solutions with different solvent proportions, aq. HEPES buffer/CH_3CN with 1:4 (v/v) and 2:3 (v/v), were used for studies. These solutions were prepared, stored under dark conditions and used for all spectroscopic studies after an appropriate dilution. A 1.0×10^{-3} M solution of different polynucleotides and the tetrabutylammonioum salt of the respective anions were prepared in the same solvent mixture. Solutions of complex **L_1Zn** were further diluted for optical spectral studies and the effective final concentration was adjusted to 2.15×10^{-5} M; while the effective concentrations of the different analyte (anions) was adjusted to 8.0×10^{-4} M.

Luminescence Study: Two different standard solutions were used for the luminescence titration studies. Different stock solutions of **L_1Zn** in an aq. HEPES buffer/CH_3CN (1:4 (v/v), pH = 7.4) and an aq. HEPES buffer/CH_3CN (2:3 (v/v), pH = 7.4) medium were prepared and stored in the dark. For all measurements, λ_{ext} = 315 nm was used (excitation and emission slit width of 3/3 nm). The initial concentration of **L_1Zn** for both stock solutions was maintained at 1.07×10^{-4} M. The first stock solution [aq. HEPES buffer/CH_3CN (1:4, v/v)] was used for recording the changes in the spectral pattern for **L_1Zn** in the presence of various added anions (F^-, Cl^-, Br^-, I^-, NO_3^-, CH_3COO^-, $C_6H_5COO^-$, SO_4^{2-}, HSO_4^-, $HP_2O_7^{3-}$, $H_2PO_4^-$) with an effective [**L_1Zn**] = 2.15×10^{-5} M. The second stock solution [aq. HEPES buffer/CH_3CN, 2:3 (v/v)] was used to record spectra with PPi and the different nucleotides (ATP, CTP, AMP, ADP), while the effective concentrations were 8.0×10^{-4} M and 2.15×10^{-5} M for the anionic analyte and **L_1Zn**, respectively.

Two different sets of fluorescence titrations were carried out. For the first set of titrations a stock solution of the **L_1Zn** [in an aq. HEPES buffer/CH_3CN (1:4, v/v) medium] was used after appropriate dilution. Tetrabutylammonium (TBA) salts of the respective anions ([A] = 1.0×10^{-3} M; "A" stands for anion) were prepared in the same solvent medium. All titration experiments were performed using 2.15×10^{-5} M solutions of complex **L_1Zn** and varying [$HP_2O_7^{3-}$] (0–2.0×10^{-4} M). The second set of titrations were carried out using an aq. HEPES buffer/CH_3CN (pH = 7.4) (2:3, v/v) solution, while maintaining [**L_1Zn**] = 2.15×10^{-5} M. A stock solution of [A] = 2.0×10^{-3} M for the respective nucleotides (ADP, AMP) was prepared in an aq. HEPES buffer/CH_3CN (pH = 7.4) (2:3, v/v) medium. For this set of titrations a varying [A] (0–1.0×10^{-3} M) (A is AMP or ADP) was used. Binding constants were calculated from fluorescence intensities using the method described by Lehrer, Fashman and Chipman et al.[24] According to this procedure fluorescence intensities (F_0, F_x and F_α) are related to the analyte concentration [A] through Equations (1) and (2), where F_0 and F_α are the relative fluorescence intensities at the initial point and saturation point, respectively, and F_x is the fluorescence intensity at a certain concentration of added analyte [A].

$$\{F_0 - F_x\}/(\{F_x - F_\alpha\}) = ([A]^n)/K_d{}^n \quad (1)$$

$$\log[\{F_0 - F_x\}/(\{F_x - F_\alpha\}] = n\log[A] - n\log K_d \quad (2)$$

The binding constant K_b is obtained by plotting $\log[(F_0 - F_x)/(F_x - F_\alpha)]$ vs. $\log[A]$. The slope of the double-logarithmic plot obtained from the experimental data is the number of binding sites or stoichiometry (n); whereas the value of $\log([A])$ at $\log[(F_0 - F_x)/(F_x - F_\alpha)] = 0$ gives $\log K_d$. The reciprocal of K_d is the binding constant K_b.

Computational Methodology: The calculations were performed from a generalized gradient approximation (GGA)[25] using the BLYP functional[26] integrated in the density functional program DMol3 (version 4.1.2) of Accelrys Inc.[27] The physical wave functions were expanded in terms of numerical basis sets. We used a DNP double-numerical polarized basis set that is comparable to the 6-31G** basis set. The conductor-like screening model (COSMO) was employed for solvent calculations.[28] The molecular electrostatic potential (MESP) was calculated using Equation (3), where Z_A is the charge on nucleus "A" located at distance R_A and $\rho(r')$ is the electron density.[29]

$$V(r) = \sum_A \frac{Z_A}{|R_A - r|} - \int \frac{\rho(r')dr'}{|r' - r|} \quad (3)$$

In general, electron-dense regions are expected to show high negative MESP whereas electron deficient regions are characterized by positive MESP.[30] The most negative valued point (V_{min}) in electron-rich regions and the most positive values point (V_{max}) can be obtained from the MESP topography calculation.[31] Molecular electrostatic potentials (MESP) were calculated for $HP_2O_7^{3-}$, monoanionic form of AMP and ADP at the BLYP/6-31G** level in both an acetonitrile and water medium using the Gaussian 03 program.[32]

Synthesis of L_1: 4′-[4-(Bromomethyl)phenyl]-2,2′:6′,2′′-terpyridine (0.51 g, 1.263 mmol), 7-hydroxy-4-methylcoumarin (0.222 g, 1.263 mmol), K_2CO_3 (0.262 g, 1.894 mmol) and 18-crown-6 (0.034 g, 0.1 equiv.) in dry acetone (100 mL) were refluxed under a dinitrogen atmosphere with continuous stirring for 48 h in an appropriate round-bottomed flask. The reaction mixture was then cooled to room temperature and poured into ca. 80 mL water. A precipitate was obtained and this was then filtered. The residue was washed with ca. 50 mL water and dried over P_2O_5. The desired product was further purified by column chromatography using silica gel as a stationary phase and $CH_3OH/CHCl_3$ (2:98, v/v) as the eluent. The major fraction was collected and after drying under reduced pressure pure product was isolated as a white solid; yield 0.21 g, 44%. ^{1}H NMR (500 MHz, $CDCl_3$, 25 °C, TMS): δ = 8.74–7.72 (m, 4 H, ArH), 8.68 (d, J = 8 Hz, 2 H, ArH), 7.94 (d, J = 8 Hz, 2 H, ArH), 7.91–7.87 (m, 2 H, ArH) 7.58 (d, J = 8 Hz, 2 H, ArH), 7.52 (d, J = 9 Hz, 1 H, ArH), 7.37 (d, J = 7.5 Hz, 2 H, ArH), 6.96 (d, J = 6 Hz, 1 H, ArH), 6.93 (s, 1 H, ArH), 6.18 (s, 1

H, ArH), 5.21 (s, 2 H, $–CH_2$), 2.41 (s, 3 H, –CH3) ppm. FTIR (KBr): $\tilde{\nu}_{max}$ = 3051, 2924, 1727, 1611, 1387, 1266, 1145, 1069, 835, 789 cm^{-1}. ESI-Ms: (*m*/*z*) = 498.48 (M^+, 15%), 521.45 ($M^+ + Na^+$, 100%). $C_{32}H_{23}N_3O_3$ (497.55): calcd. C 77.25, H 4.66, N 8.45; found C 77.3, H 4.7, N 8.4.

L_1Zn: L_1 was found to have a limited solubility in methanol. Thus, **L_1** (0.10 g, 0.201 mmol) was dissolved in a minimum volume of $CHCl_3$ (ca. 5 mL). Methanol (30 mL) was then added to this solution. $Zn(ClO_4)_2·6H_2O$ (0.075 g, 0.301 mmol), dissolved in water (5 ml), was added to this in a dropwise manner and the reaction mixture was allowed to stir at room temperature for 24 h. The desired compound was then allowed to precipitate in a pure form by slow evaporation of the solvent at room temperature. The precipitate thus obtained was filtered, washed with cold water and dried over P_2O_5; yield 0.107 g, 70%. ^1H NMR (200 MHz, CD_3OD + D_2O, 25 °C, TMS): δ = 9.03 (s, 2 H, ArH), 8.82 (d, *J* = 7.8 Hz, 2 H, ArH), 8.24–8.16 (m, 4 H, ArH), 7.97 (m, 2 H, ArH), 7.88–7.79 (m, 4 H, ArH), 7.69 (d, *J* = 8.6 Hz, 1 H, ArH), 7.18 (d, *J* = 6.4 Hz, 1 H, ArH), 6.98 (s, 1 H, ArH), 6.62 (s, 1 H, ArH), 5.37 (s, 2 H, $–CH_2$), 2.48 (s, 3 H, $–CH_3$) ppm. FTIR (KBr): $\tilde{\nu}_{max}$ = 3477, 3075, 2338, 1715, 1610, 1476, 1431, 1389, 1266, 1092, 794, 623 cm^{-1}. ESI-Ms: (*m*/*z*) = 660 ([**L_1Zn** ClO_4]$^+$, 100%), 836 {[**L_1·Zn** $(ClO_4)_2$ + $2H_2O$ + K^+], 20%}. {[**L_1Zn** $(H_2O)_2$]$(ClO_4)_2$}; $C_{32}H_{27}C_{l2}N_3O_{13}Zn$ (797.86): calcd. C 48.17, H 3.41, N 5.27; found C 48.1, H 3.4, N 5.1.

Supporting Information (see footnote on the first page of this article): Synthesis of precursors and intermediates, various absorption, emission and excitation spectra, ESI-Ms spectra of **L_1Zn**, frontier orbitals for **L_1Zn**–PPi and time resolved emission data.

Acknowledgments

Authors thank the Department of Science and Technology and Council of Scientific and Industrial Research (CSIR), India for supporting this research. P. D. and A. G. thank the CSIR for a Sr. Research Fellowship. M. K. K. thanks the University Grants Commission (UGC), New Delhi for a Sr. Research Fellowship. V. R. thanks the Department of Bio Technology (DBT), India for a research fellowship. A. D. thanks Dr. P. K. Ghosh, Director, CSMCRI for his encouragement.

[1] a) G. V. Zyryanov, M. A. Palacios, P. Anzenbacher Jr., *Angew. Chem. Int. Ed.* **2007**, *46*, 7849; b) M. W. Hosseini, A. John Blacker, J. M. Lehn, *J. Am. Chem. Soc.* **1990**, *112*, 3896; c) W. N. Lipscomb, N. Starter, *Chem. Rev.* **1996**, *96*, 2375; d) J. M. Berg, L. Stryer, J. L. Tymoczko, *Biochemistry* 5th Ed., W. H. Freeman, New York **2002**; e) J. S. Seo, N. D. Sung, R. C. Hynes, J. Chin, *Inorg. Chem.* **1996**, *35*, 7472; f) Z. Xu, N. J. Singh, J. Lim, J. Pan, H. N. Kim, S. Park, K. S. Kim, J. Yoon, *J. Am. Chem. Soc.* **2009**, *131*, 15528.

[2] a) R. Martinez-Manez, F. Sancenon, *Chem. Rev.* **2003**, *103*, 4419; b) S. K. Kim, D. H. Lee, J. Hong, J. Yoon, *Acc. Chem. Res. Acc. Chem. Research.* **2009**, *42*, 23; c) G. Ambrosi, M. Formica, V. Fusi, A. Guerri, E. Macedi, M. Micheloni, P. Paoli, R. Pontellini, P. Rossi, *Inorg. Chem.* **2009**, *48*, 5901; d) E. Climent, R. Casasus, M. D. Marcos, R. Martinez-Manez, F. Sancenon, J. Soto, *Dalton Trans.* **2009**, 4806; e) E. A. Katayev, Y. A. Ustynyuk, J. L. Sessler, *Coord. Chem. Rev.* **2006**, *250*, 3004; f) E. O'Neil, B. D. Smith, *Coord. Chem. Rev.* **2006**, *250*, 3068; g) P. Molenveld, J. F. J. Engbersen, D. N. Reinhoudt, *Chem. Soc. Rev.* **2000**, *29*, 75.

[3] a) A. D. Silva, H. Q. N. Gunaratne, T. Gunnlaugsson, A. J. M. Huxley, C. P. McCoy, J. T. Radamacher, T. E. Roice, *Chem. Rev.* **1997**, *36*, 2081; b) F. Sancenon, A. B. Descalzo, M. M. Manez, M. A. Miranda, J. Soto, *Angew. Chem. Int. Ed.* **2001**, *40*, 2640; c) X. Zhao, Y. Liu, K. S. Schanze, *Chem. Commun.* **2007**, 2914; d) T. Romero, A. Caballero, A. Tarraga, P. Molina, *Org. Lett.* **2009**, *5*, 3466; e) S. K. Kim, N. J. Singh, J. Kwon, I. C. Hwang, S. J. Park, K. S. Kimb, J. Yoon, *Tetrahedron* **2006**, *62*, 6065.

[4] a) C. Marquez, U. Pischel, W. M. Nau, *Org. Lett.* **2003**, *5*, 3911; b) M. K. Coggins, A. M. Parker, A. Mangalum, G. A. Galdamez, R. C. Smith, *Eur. J. Org. Chem.* **2009**, 343; c) A. Ojida, Y. Mito-oka, M. Inoue, I. Hamachi, *J. Am. Chem. Soc.* **2002**, *124*, 6256; d) A. Ojida, Y. Mito-oka, K. Sada, I. Hamachi, *J. Am. Chem. Soc.* **2004**, *126*, 2454; e) T. Gunnlaugsson, A. P. Davis, J. E. O'Brien, M. Glynn, *Org. Lett.* **2002**, *4*, 2249; f) P. P. Neelakandan, M. Hariharan, D. Ramaiah, *Org. Lett.* **2005**, *7*, 5765.

[5] a) P. Nyrén, *Anal. Biochem.* **1987**, *167*, 235; b) T. Tabary, L. J. Ju, *Immunol. Methods* **1992**, *156*, 55; c) D. Mulkerrins, A. D. W. Dobson, E. Colleran, *Environ. Int.* **2004**, *30*, 249.

[6] a) D. J. McCarty, *Arthritis Rheum.* **1976**, *19*, 275; b) A. Caswell, D. F. Guilland-Cumming, P. R. Hearn, M. K. McGuire, R. G. Russell, *Ann. Rheum. Dis.* **1983**, *42*, 27; c) M. Doherty, *Ann. Rheum. Dis.* **1983**, *42*, 38.

[7] a) H.-W. Rhee, C.-R. Lee, S.-H. Cho, M.-R. Song, M. Cashel, H. E. Choy, Y.-J. Seok, J.-I. Hong, *J. Am. Chem. Soc.* **2008**, *130*, 784; b) H.-W. Rhee, H.-Y. Choi, K. Han, J.-I. Hong, *J. Am. Chem. Soc.* **2007**, *129*, 4524.

[8] M. Ronaghi, S. Karamohamed, B. Pettersson, M. Uhlén, P. Nyrén, *Anal. Biochem.* **1996**, *242*, 84.

[9] S. Xu, M. He, H. Yu, X. Cai, X. Tan, B. Lu, B. Shu, *Anal. Biochem.* **2001**, *299*, 188.

[10] a) D. H. Lee, J. H. Im, S. U. Son, Y. K. Chung, J.-I. Hong, *J. Am. Chem. Soc.* **2003**, *125*, 7752; b) X. Chen, M. J. Jou, J. Yoon, *Org. Lett.* **2009**, *11*, 2181; c) H. N. Lee, Z. Xu, S. Kyung, K. Kim, M. K. Swamy, Y. Kim, S.-J. Kim, J. Yoon, *J. Am. Chem. Soc.* **2007**, *129*, 3828; d) A. J. Moro, P. J. Cywinski, S. Korsten, G. J. Mohr, *Chem. Commun.* **2010**, *46*, 1085; e) Z. Kejík, K. Záruba, D. Michalík, J. Ebek, J. Dian, S. Pataridis, K. Volka, V. Král, *Chem. Commun.* **2006**, 1533; f) B. A. Smith, W. J. Akers, W. M. Leevy, A. J. Lampkins, S. Xiao, W. Wolter, M. A. Suckow, S. Achilefu, B. D. Smith, *J. Am. Chem. Soc.* **2010**, *132*, 67, and references cited therein; g) W. M. Leevy, S. T. Gammon, H. Jiang, D. J. Maxwell, E. N. Jackson, M. Marquez, D. P. Worms, B. D. Smith, *J. Am. Chem. Soc.* **2006**, *128*, 16476; h) D. H. Lee, S. Y. Kim, J. I. Hong, *Tetrahedron Lett.* **2007**, *48*, 4477; i) H. N. Lee, K. M. K. Swamy, S. K. Kim, J. Y. Kwon, Y. Kim, S. J. Kim, Y. J. Yoon, J. Yoon, *Org. Lett.* **2007**, *9*, 243; j) H. K. Cho, D. H. Lee, J. I. Hong, *Chem. Commun.* **2005**, 1690; k) K. M. K. Swamy, S. Y. Kwon, H. N. Lee, S. M. S. Kumar, J. S. Kim, J. Yoon, *Tetrahedron Lett.* **2007**, *48*, 8683.

[11] a) D. H. Lee, S. Y. Kim, J.-I. Hong, *Angew. Chem. Int. Ed.* **2004**, *43*, 4777; b) M. S. Han, D. H. Kim, *Angew. Chem. Int. Ed.* **2002**, *41*, 3809; c) A. D. Jose, S. Mishra, A. Ghosh, A. Shrivastav, S. K. Mishra, A. Das, *Org. Lett.* **2007**, *9*, 1979; d) A. Ghosh, A. Shrivastav, A. D. Jose, S. K. Mishra, C. K. Chandrakanth, S. Mishra, A. Das, *Anal. Chem.* **2008**, *80*, 5312; e) A. Ojida, S. Park, Y. Mito-oka, I. Hamachi, *Tetrahedron Lett.* **2002**, *43*, 6193; f) J. Wongkongkatep, Y. Miyahara, A. Ojida, I. Hamachi, *Angew. Chem. Int. Ed.* **2006**, *45*, 665; g) A. Ojida, I. Takashima, T. Kohira, H. Nonaka, I. Hamachi, *J. Am. Chem. Soc.* **2008**, *130*, 12095, and references cited therein; h) D. H. Lee, J. H. Im, S. U. Son, Y. K. Chung, J.-I. Hong, *J. Am. Chem. Soc.* **2003**, *125*, 7752; i) X. Haung, Z. Guo, W. Zhu, Y. Xie, H. Tian, *Chem. Commun.* **2008**, 5143; j) M. J. Kim, K. M. K. Swamy, K. M. Lee, A. R. Jagdale, Y. Kim, S. J. Kim, K. H. Yoo, J. Yoon, *Chem. Commun.* **2009**, 7215.

[12] a) D. A. Jose, S. Stadlbauer, B. Kçnig, *Chem. Eur. J.* **2009**, *15*, 7404; b) S. Aoki, M. Zulkefeli, M. Shiro, M. Kohsako, K. Takeda, E. Kimura, *J. Am. Chem. Soc.* **2005**, *127*, 9129; c) S.

Khatua, S. H. Choi, J. Lee, K. Kim, Y. Do, D. G. Churchill, *Inorg. Chem.* **2009**, *29*, 299.
[13] a) S. Mizukami, T. Nagano, Y. Urano, A. Odani, K. Kikuchi, *J. Am. Chem. Soc.* **2002**, *124*, 3920; b) J. Gao, J. H. Reibenspies, A. E. Martell, *Org. Biomol. Chem.* **2003**, *1*, 42429; c) A. E. Martell, R. J. Motekaitis, *Inorg. Chim. Acta* **1996**, *251*, 365.
[14] a) M. A. Hayes, C. Meckel, E. Schatz, M. D. Ward, *J. Chem. Soc., Dalton Trans.* **1992**, 703; b) S. M. Treffert-Ziemils, J. Golus, D. P. Strommen, I. P. Kincaid, *Inorg. Chem.* **1993**, *32*, 3890; c) F. Kröhnke, K. F. Gross, *Chem. Ber.* **1959**, *92*, 22; d) B. Whitlle, N. S. Everest, C. Howard, M. D. Ward, *Inorg. Chem.* **1995**, *34*, 2025; e) J.-P. Collin, S. Guillerez, J.-P. Sauvage, F. Barigelletti, L. De Cola, L. Flamigni, V. Balzani, *Inorg. Chem.* **1991**, *30*, 4230.
[15] J. Wang, G. S. Hanan, *Synlett* **2005**, 1251.
[16] F. Tessore, D. Roberto, R. Ugo, M. Pizzotti, *Inorg. Chem.* **2005**, *44*, 8967.
[17] M. Aydinli, M. Tutas, B. Atasoy, A. O. Bozdemir, *Reactive Funct. Polymers.* **2005**, *65*, 317.
[18] J. S. S. De Melo, R. S. Becker, A. L. Macanita, *J. Phys. Chem.* **1994**, *98*, 6054.
[19] a) V. Amendola, D. E. Gomez, L. Fabbrizzi, M. Licchelli, *Acc. Chem. Res. Acc. Chem. Research.* **2006**, *39*, 343; b) A. Ghosh, D. A. Jose, A. Das, B. Ganguly, *J. Mol. Model.* **2010**, *16*, 1441.
[20] D. M. Y. Alves, *Mensaje Bioquimico* **2004**, vol. XVVII.
[21] a) A. K. Nair, P. N. Prakash, D. Ramaiah, *Chem. Commun.* **2009**, 6352; b) P. P. Neelakandan, M. Hariharan, D. Ramaiah, *J. Am. Chem. Soc.* **2006**, *128*, 11334; c) E. A. Meyer, R. K. Castellano, F. Diederich, *Angew. Chem. Int. Ed.* **2003**, *42*, 8407; d) H.-J. Schneider, *Angew. Chem. Int. Ed. Engl.* **1991**, *30*, 1417.
[22] a) E. Kimura, M. Kodama, T. J. Yatsunami, *J. Am. Chem. Soc.* **1982**, *104*, 3182; b) M. S. Han, D. H. Kim, *Bioorg. Med. Chem. Lett.* **2003**, *13*, 1079.
[23] K. D. Surya, R. A. Gibbs, *Synthesis* **2005**, 1231.
[24] a) S. S. Lehrer, G. D. Fashman, *Biochem. Biophys. Res. Commun.* **1996**, 133; b) D. M. Chipman, V. Grisaro, N. Shanon, *J. Biol. Chem.* **1967**, *242*, 4388.
[25] J. P. Perdew, J. A. Chevary, S. H. Vosko, K. A. Jackson, M. R. Pederson, D. J. Singh, C. Fiolhais, *Phys. Rev. B* **1992**, *46*, 6671.
[26] a) A. D. Becke, *J. Chem. Phys.* **1997**, *107*, 8554; b) C. Lee, W. Yang, R. G. Parr, *Phys. ReV. B* **1988**, *37*, 785.
[27] B. Delley, *J. Chem. Phys.* **2000**, *113*, 7756.
[28] a) F. J. Neese, *Chem. Ph.* **2003**, *119*, 9428; b) F. Neese, *Curr. Opin. Cell Biol.* **2003**, *7*, 125.
[29] P. Politzer, J. S. Murray, in: *Reviews in Computational Chemistry* (Eds.: K. B. Lipkowitz, D. B. Boyd), VCH Publishers, New York, **1991**, vol. 2, chapter 7.
[30] a) R. K. Pathak, S. R. Gadre, *J. Chem. Phys.* **1990**, *93*, 1770; b) T. Brinck, J. S. Murray, P. Politzer, *Mol. Phys.* **1992**, *76*, 609; c) J. S. Murray, P. J. Politzer, *Mol. Struct. (Theochem)* **1998**, *425*, 107.
[31] a) G. Trogdon, J. S. Murray, M. C. Concha, P. Politzer, *J. Mol. Model.* **2006**, *13*, 313; b) P. Politzer, in: *Chemical Applications of Atomic and Molecular Electrostatic Potentials* (Eds.: P. Politzer, D. G. Truhlar), Plenum, New York, **1981**; c) J. S. Murray, P. Politzer, *Chem. Phys. Lett.* **1988**, *152*, 364; d) M. Haeberlein, J. S. Murray, T. Brinck, P. Politzer, *Can. J. Chem.* **1992**, *70*, 2209; e) J. M. Wiener, M. E. Grice, J. S. Murray, P. Politzer, *J. Chem. Phys.* **1996**, *104*, 5109.
[32] M. J. Frisch, G. W. Trucks, H. B. Schlegel, G. E. Scuseria, M. A. Robb, J. R. J. Cheeseman Jr., A. Montgomery, T. Vreven, K. N. Kudin, J. C. Burant, J. M. Millam, S. S. Iyengar, J. Tomasi, V. Barone, B. Mennucci, M. Cossi, G. Scalmani, N. Rega, A. G. Petersson, H. Nakatsuji, M. Hada, M. Ehara, K. Toyota, R. Fukuda, J. Hasegawa, M. Ishida, T. Nakajima, Y. Honda, O. Kitao, H. Nakai, M. Klene, X. Li, J. E. Knox, H. P. Hratchian, J. B. Cross, V. Bakken, C. Adamo, J. Jaramillo, R. Gomperts, R. E. Stratmann, O. Yazyev, A. J. Austin, R. Cammi, C. Pomelli, J. W. Ochterski, P. Y. Ayala, K. Morokuma, G. A. Voth, P. Salvador, J. J. Dannenberg, V. G. Zakrzewski, S. Dapprich, A. D. Daniels, M. C. Strain, O. Farkas, D. K. Malick, A. D. Rabuck, K. Raghavachari, J. B. Foresman, J. V. Ortiz, Q. Cui, A. G. Baboul, S. Clifford, J. Cioslowski, B. B. Stefanov, G. Liu, A. Liashenko, P. Piskorz, I. Komaromi, R. L. Martin, D. J. Fox, T. Keith, M. A. Al-Laham, C. Y. Peng, A. Nanayakkara, M. Challacombe, P. M. W. Gill, B. Johnson, W. Chen, M. W. Wong, C. Gonzalez, J. A. Pople, *Gaussian 03*, Revision E. 01, Gaussian, Inc. Wallingford CT, **2004**.

Received: February 4, 2011
Published Online: June 1, 2011

